How Does the Plasmonic Enhancement on Molecular Absorption Depend on the Energy Gap between Molecular Excitation and Plasmon Mode: A Mixed TDDFT/FDTD Investigation

Jin Sun[1], Guang Li[1] and WanZhen Liang[2,*]

[1] *School of Physics and Materials Science, Anhui University, Hefei 230601, People's Republic of China*

[2] *State Key Laboratory of Physical Chemistry of Solid Surfaces, Collaborative Innovation Center of Chemistry for Energy Materials, and Department of Chemistry, College of Chemistry and Chemical Engineering, Xiamen University, Xiamen 361005, People's Republic of China*

(Dated: May 28, 2015)

The surface near-field of NPs in time-domain

Firstly, we investigate the total electric field near a silver sphere whose center is also the center of the cubic simulation box $(0, 0, 0)$. The incident laser pulse is assumed to have a polarization direction along the x axis. Compared with the duration of incident laser pulse, the durations of all the total electric field are extended as shown in Fig.S1.

Fig.S1(a) shows the field at the point (6,0,0), (11,0,0) and (13,0,0) yielded by Ag spheres with different radii of $R = 5$, 10, 12 nm, respectively, corresponding the separation distance $L = 1nm$. It is found that the sizes of small Ag NPs have a significant influence on the surface near-field. The larger the silver sphere size, the stronger the near-field. The inset of Fig.S1(a) shows a linear d ependence of the maximum near-field intensity to the silver sphere radius for the small Ag nanoparticle at about $t = 10$ fs. Contrary to the change of the field intensity vs NP's radius, we find that as the NP's radius increases, the duration of electric field becomes shorter. And these competitive changes will lead to a red-shift of plasmon bands which we show in the paper.

In order to study the decay factor of the near-field with the separation distance to the sphere surface, we calculate the total electric fields at different points corresponding to

a surface separation distance of $L = 1$, 3 and 5 nm, respectively (see Fig.S1(c)). The observation points are set at x axis as shown in the inset of Fig.S1(b). The localized field decays to zero quickly as the separation distance from Ag sphere surface increases. The maximum intensity of field decreases exponentially and the duration of field becomes shorter as L increases.

The components of total electric field near Ag NPs in three coordinate directions are different. Fig.S1(d) displays the x-, y- and z-components of the electric field at $L = 1$ nm. The results indicate that the component of field along the polarization direction of incident pulse is much stronger than the other two components. It is that $E_{total,y}$ and $E_{total,z}$ are negligible small comparing with the $E_{total,x}$.

For a spherical NP with radius R in vacuo $P(\omega)/E_0(\omega) = \epsilon_0\chi(\omega)R^3$, which corresponds to $\epsilon_0\frac{\epsilon_p(\omega)-\epsilon_0}{\epsilon_p(\omega)+2\epsilon_0}R^3$ in classical theory, the field-induced polarization on NPs yields the strong surface near-field. If the polarization can be identified by a dipole, the field yielded by the induced dipole is proportional to $s_\sigma P/(R+L)^3$ with $s_\sigma = 2(-1)$ for electric field polarizations $\sigma = x(y, z)$. Here the x direction corresponds to the external-field polarization direction. From the classical model, it is apparent that the surface localized field yielded by the NP sphere is dependent on the NP's radius, the position of the observation point. The larger the radius R, the stronger the localized field. The smaller the separation distance L, the stronger the localized field. The results from our FDTD simulation and those from the classical theory are quantitatively consistent although there exists the explicit difference.

Secondly, we calculate the localized field generated by two Ag NPs. The Ag dimer axis is set to normal and perpendicular to the polarization direction of incident field, respectively. Two silver spheres have the same radii of $R = 5$ nm and the distance between two sphere centers is 12 nm. A comparison of the field intensities is shown on Fig.S2. For the Ag dimer along x axis, the electric field observed at $(0, 0, 0)$. The crevice between NP dimers leads to the field raising from about $2V/m$ to about $6V/m$. Besides, the duration of field is evidently extended. For the Ag dimer along y axis, the observed point is chosen at $(6, 6, 0)$. The electric field at observed point is displayed in Fig.S2. Explicitly, there isn't observable difference from the electric field of one Ag NP.

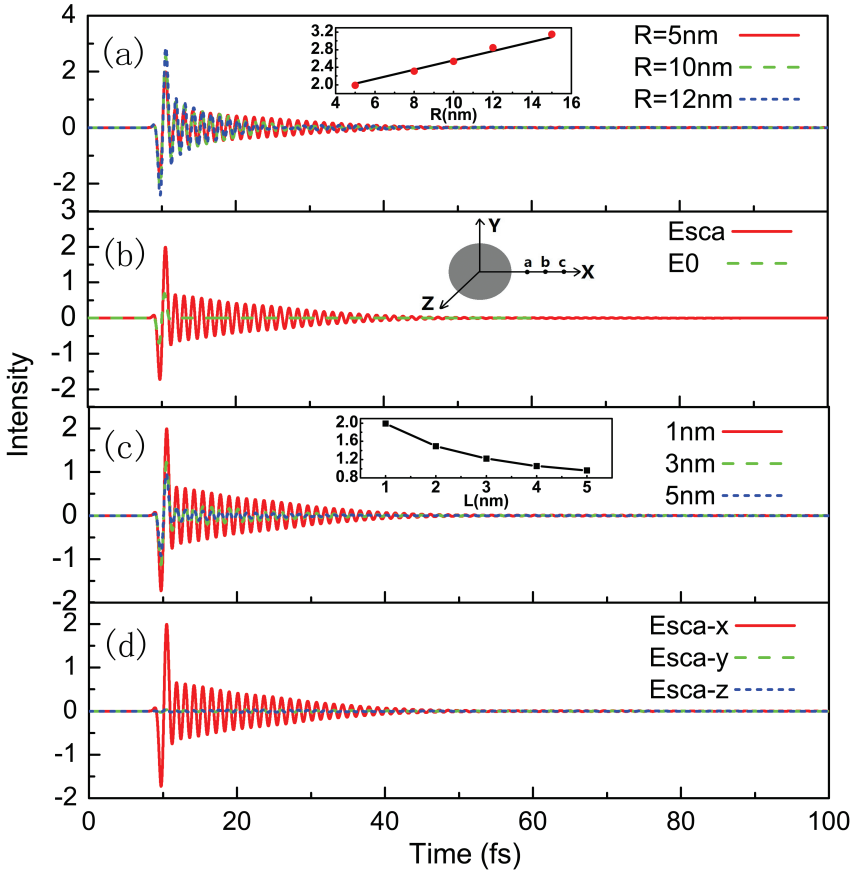

FIG. S1: (a) The total electric fields near silver spheres with different sphere radii at the observed points $(6,0,0)$, $(11,0,0)$ and $(13,0,0)$ in time domain. (b) The total electric field near 5 nm radius silver sphere observed at $(6,0,0)$. A comparison is made for the incident laser pulse. (c) The total electric field of 5 nm radius silver sphere observed at $(6,0,0)$, $(8,0,0)$ and $(10,0,0)$. (d) The x-, y- and z-components of total electric field of 5 nm radius silver sphere at $(6,0,0)$.

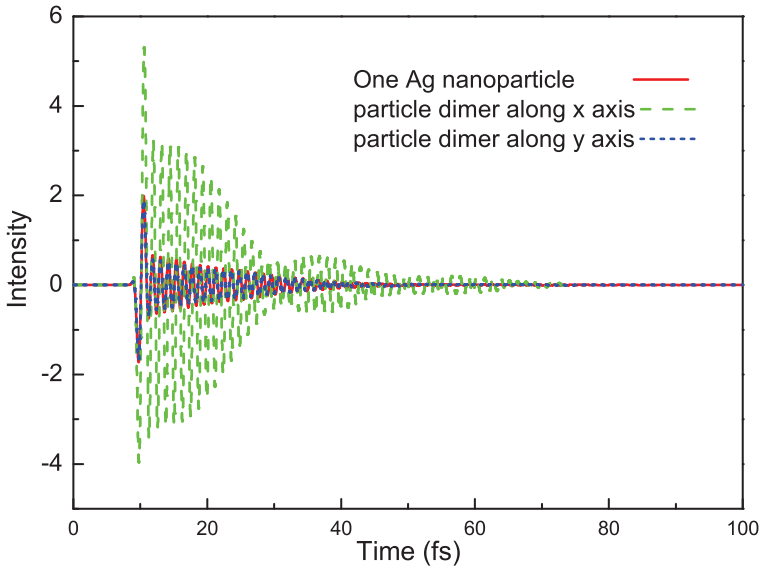

FIG. S2: The total electric fields at $(0, 0, 0)$ of silver sphere dimer arrayed along x axis and at $(6, 6, 0)$ of silver sphere dimer arrayed along y axis. The field of one silver sphere with $R = 5$ nm at $(6, 0, 0)$ is shown for the comparison (the red line).

TABLE I: The vertical excitation energies and transition dipole moments of MC and SP calculated by TD-B3LYP/6-31G within Q-Chem package. Here f denotes the oscillator strength and VE denotes the vertical excitation energy.

MC					SP				
	Transition dipole moments					Transition dipole moments			
VE(eV)	X	Y	Z	f	VE(eV)	X	Y	Z	f
2.5046	3.2215	0.2411	-0.0003	0.6404	2.6041	0.4639	-0.0041	0.0395	0.0138
3.3309	2.2764	-0.1183	-0.0002	0.4240	3.4074	0.1236	-0.1456	-0.0157	0.0031
3.5266	0.3465	-1.1378	0.0005	0.1222	3.5045	1.5007	-0.0775	-0.0559	0.1941
4.0879	0.1026	-0.0050	-0.0006	0.0011	4.0734	-0.9294	-0.0130	0.0215	0.0863
4.1024	-0.6953	0.2786	-0.0001	0.0564	4.3610	-1.2766	-0.5819	-0.3204	0.2213
4.2129	-0.9423	0.1718	0.0010	0.0947	4.7659	0.0975	0.3310	-0.0691	0.0145
4.2524	0.3245	-0.1844	-0.0009	0.0145	4.7995	-0.3028	0.2789	-0.3047	0.0308
4.3345	-0.7194	-0.0052	0.0001	0.0550	4.9151	-0.1590	-0.0342	0.0313	0.0033
4.5928	0.6002	-0.0094	0.0027	0.0405					